

CONSTRAINTS ON THE PROCESS THAT REGULATES THE GROWTH OF SUPERMASSIVE BLACK HOLES BASED ON THE INTRINSIC SCATTER IN THE $M_{\text{BH}}-\sigma$ RELATION

J. STUART B. WYITHE¹, ABRAHAM LOEB²
 swyithe@physics.unimelb.edu.au; aloeb@cfa.harvard.edu

Draft version September 25, 2018

ABSTRACT

We show that the observed scatter in the relations between the mass of supermassive black holes (SMBHs), M_{bh} , and the velocity dispersion σ_{sph} or mass M_{sph} of their host spheroid, place interesting constraints on the process that regulates SMBH growth in galaxies. When combined with the observed properties of early-type SDSS galaxies, the observed intrinsic scatters imply that SMBH growth is regulated by the spheroid velocity dispersion rather than its mass. The $M_{\text{bh}}-M_{\text{sph}}$ relation is therefore a by-product of a more fundamental $M_{\text{bh}}-\sigma_{\text{sph}}$ relation. We construct a theoretical model for the scatter among baryon modified dark matter halo profiles, out of which we generate a population of spheroid hosts and show that these naturally lead to a relation between effective radius and velocity dispersion of the form $R_{\text{sph}} \approx 6\text{kpc}(\sigma_{\text{sph}}/200\text{km s}^{-1})^{1.5}$ with a scatter of $\sim 0.2\text{dex}$, in agreement with the corresponding projection of the fundamental plane for early type galaxies in SDSS. At the redshift of formation, our model predicts the minimum scatter that SMBHs can have at fixed velocity dispersion or spheroid mass under different formation scenarios. We also estimate the additional scatter that is introduced into these relations through collisionless mergers of purely stellar spheroids at $z < 1$. We find that the observed scatter in the $M_{\text{bh}}-\sigma_{\text{sph}}$ and $M_{\text{bh}}-M_{\text{sph}}$ relations preclude the properties of dark matter halos from being the governing factor in SMBH growth. The apparent relation between halo and SMBH mass is merely a reflection of the fact that massive halos tend to host massive stellar spheroids (albeit with a large scatter owing to the variance in formation histories). Finally, we show that SMBH growth governed by the properties of the host spheroid can lead to the observed values of scatter in the $M_{\text{bh}}-\sigma_{\text{sph}}$ and $M_{\text{bh}}-M_{\text{sph}}$ relations, only if the SMBH growth is limited by momentum or energy feedback *over the dynamical time* of the host spheroid.

Subject headings: cosmology: theory - galaxies: formation

1. INTRODUCTION

Supermassive black holes (SMBHs) are a ubiquitous constituent of spheroids in nearby galaxies (e.g. Kormandy & Richstone 1995). A decade ago it became apparent that the masses of SMBHs correlate with the luminosity of the host spheroid (Kormandy & Richstone 1995). Subsequently, other correlations with substantially less intrinsic scatter have been discovered. These include correlations between the SMBH mass (M_{bh}), and the mass, M_{sph} (Magorrian et al. 1998; Haering & Rix 2004), stellar velocity dispersion, σ_{sph} (Ferrarese & Merritt 2000; Gebhardt et al. 2000), and concentration (Graham et al. 2002) of its host spheroid. The tightest relation, with intrinsic scatter of $\delta \sim 0.275 \pm 0.05\text{dex}$, appears to be between SMBH mass and velocity dispersion (Tremaine et al. 2002; Wyithe 2005).

These relations must hold important clues about the astrophysics that regulates the growth of a SMBH and its impact on galaxy formation. While much attention was dedicated towards interpreting the power-law slope of the $M_{\text{bh}}-\sigma_{\text{sph}}$ relation via a slew of analytic, semi-analytic and numerical attempts to reproduce it (e.g. Silk & Rees 1998; Wyithe & Loeb 2003; King 2003; Miralda-Escude & Kollmeier 2005; Adams et al. 2003; Sazonov et al. 2005; Di Matteo et al. 2005), little attention has been directed towards interpreting the constraints that its *intrinsic scatter* might place on our understanding of SMBH

growth (Robertson et al. 2005). Moreover, agreement between data and theory is a necessary but not sufficient condition. A model that reproduces the observations is not necessarily unique. The various successful attempts to model the quasar luminosity function assuming different physical models attest to this fact. Our goals in this paper are to use the observed scatter in the $M_{\text{bh}}-\sigma_{\text{sph}}$ and $M_{\text{bh}}-M_{\text{sph}}$ relations in addition to their power-law slope as a diagnostic of SMBH formation physics, and to constrain a range of possible models of SMBH formation.

Throughout the paper we adopt the set of cosmological parameters determined by the *Wilkinson Microwave Anisotropy Probe* (WMAP, Spergel et al. 2003), namely mass density parameters of $\Omega_m = 0.27$ in matter, $\Omega_b = 0.044$ in baryons, $\Omega_\Lambda = 0.73$ in a cosmological constant, and a Hubble constant of $H_0 = 71 \text{ km s}^{-1} \text{ Mpc}^{-1}$.

2. INTRINSIC SCATTER IN THE OBSERVED $m_{\text{bh}}-\sigma_{\text{sph}}$ AND $m_{\text{bh}}-m_{\text{sph}}$ RELATIONS

Tremaine et al. (2002) have compiled a list of spheroids with reliable determinations of both SMBH mass and central velocity dispersion (defined as the luminosity weighted dispersion in a slit aperture of half length R_{sph}). These SMBHs show a tight correlation between M_{bh} and σ_{sph} (Gebhardt et al. 2000; Ferrarese & Merritt 2000). Recently, Wyithe (2005) found that the $M_{\text{bh}}-\sigma_{\text{sph}}$ relation within the sample of Tremaine et al. (2002) shows ev-

¹ University of Melbourne, Parkville, Victoria, Australia

² Astronomy department, Harvard University, 60 Garden St., Cambridge, MA 02138, USA

idence for a deviation from a pure power-law behavior, and obtained an a-posteriori probability distribution for the scatter in the relation of $\delta = 0.28 \pm 0.05$. The best-fit log-quadratic $M_{\text{bh}}-\sigma_{\text{sph}}$ takes the form

$$\log_{10}(M_{\text{bh}}) = \alpha + \beta \log_{10}(\sigma_{\text{sph}}/200\text{km/s}) + \beta_2 [\log_{10}(\sigma_{\text{sph}}/200\text{km/s})]^2, \quad (1)$$

where $\beta = 4.2 \pm 0.37$ corresponds to the traditional power-law relation and $\beta_2 = 1.6 \pm 1.3$ quantifies the departure of the local SMBH sample from a pure power-law.

A correlation has also been found between the mass of the spheroid component, M_{sph} , and the SMBH (Magorrian et al. 1998). The sample compiled by Haering & Rix (2004) (which overlaps predominantly with the Tremaine et al. 2002 sample) was studied by Wyithe (2005) who found that like the $M_{\text{bh}}-\sigma_{\text{sph}}$ relation, the $M_{\text{bh}}-M_{\text{sph}}$ relation may depart from a uniform power-law, and that the scatter in the $M_{\text{bh}}-M_{\text{sph}}$ relation is larger than in the $M_{\text{bh}}-\sigma_{\text{sph}}$ relation by 50% ($\delta_{\text{sph}} = 0.41 \pm 0.07$). The best-fit log-quadratic $M_{\text{bh}}-M_{\text{sph}}$ takes the form

$$\log_{10}(M_{\text{bh}}) = \alpha_{\text{sph}} + \beta_{\text{sph}} \log_{10}(M_{\text{sph}}/10^{11}M_{\odot}) + \beta_{2,\text{sph}} [\log_{10}(M_{\text{sph}}/10^{11}M_{\odot})]^2, \quad (2)$$

where $\beta_{\text{sph}} = 1.15 \pm 0.18$ and $\beta_{2,\text{sph}} = 1.12 \pm 0.14$.

In this paper we use the values of intrinsic scatter (δ and δ_{sph}) in the local SMBH sample to place constraints on the process that regulates SMBH growth in galaxies.

3. WHICH RELATION IS MORE FUNDAMENTAL: $m_{\text{bh}}-\sigma_{\text{sph}}$ OR $m_{\text{bh}}-m_{\text{sph}}$?

The SMBH mass is observed to correlate tightly with both σ_{sph} (Tremaine et al. 2002) and M_{sph} (Haering & Rix 2004), implying that SMBH growth is regulated by properties of the spheroid. It is therefore natural to ask *which parameter among these two is responsible for setting the SMBH mass?* We address this question empirically without specifying a mechanism for the SMBH growth.

Let us suppose first that the $M_{\text{bh}}-M_{\text{sph}}$ relation is the fundamental one. There would still be a relation between M_{bh} and σ_{sph} since M_{sph} and σ_{sph} are related. Bernardi et al. (2003) have compiled values of R_{sph} , and σ_{sph} for the sample of early-type galaxies in the SDSS. We can generate a sub-sample of galaxies within a narrow range of σ_{sph} and find the dynamical mass $M_{\text{sph}} = V_{\text{sph}}^2 R_{\text{sph}}/G = 2\sigma_{\text{sph}}^2 R_{\text{sph}}/G$ for each, where V_{sph} is the circular velocity at R_{sph} and we have assumed an isotropic velocity dispersion $\sigma_{\text{sph}} = V_{\text{sph}}/\sqrt{2}$. We can then use the observed relation $M_{\text{bh}} \propto M_{\text{sph}}$ with its intrinsic scatter of $\delta_{\text{sph}} = 0.41 \pm 0.07$, to find the corresponding scatter in the $M_{\text{bh}}-\sigma_{\text{sph}}$ relation. The resulting distributions of residuals in the SMBH mass are plotted on the left panel of Figure 1, together with the 1-sigma range in the observed scatter (grey region) of the $M_{\text{bh}}-\sigma_{\text{sph}}$ relation. If the $M_{\text{bh}}-M_{\text{sph}}$ relation were fundamental, then the scatter in the $M_{\text{bh}}-\sigma_{\text{sph}}$ relation would have been $\delta = 0.46\text{dex}$, well in excess of the observed value $\delta = 0.275 \pm 0.05$. This implies that the $M_{\text{bh}}-M_{\text{sph}}$ relation is not fundamental.

On the other hand if we suppose that it is the $M_{\text{bh}}-\sigma_{\text{sph}}$ relation that is fundamental, then there would still be a relation between M_{bh} and M_{sph} . We generate a sub-sample of galaxies from Bernardi et al. (2003) with $M_{\text{sph}} =$

$2\sigma_{\text{sph}}^2 R_{\text{sph}}/G$ in a narrow range near $M_{\text{sph}} = 10^{11}M_{\odot}$. We can then use the observed $M_{\text{bh}}-\sigma_{\text{sph}}$ relation (with intrinsic scatter $\delta = 0.275 \pm 0.05$) to find the corresponding scatter in the $M_{\text{bh}}-M_{\text{sph}}$ relation. The resulting distributions of residuals in SMBH mass are plotted in the right hand panel of Figure 1, together with the 1-sigma range in the observed scatter (grey region) of the $M_{\text{bh}}-M_{\text{sph}}$ relation. If the $M_{\text{bh}}-\sigma_{\text{sph}}$ relation is fundamental, then the scatter in the $M_{\text{bh}}-M_{\text{sph}}$ relation should be $\delta_{\text{sph}} = 0.40\text{dex}$, in good agreement with the observed value $\delta_{\text{sph}} = 0.41 \pm 0.07$. This implies that the $M_{\text{bh}}-\sigma_{\text{sph}}$ relation is more fundamental than the $M_{\text{bh}}-M_{\text{sph}}$ relation, with the latter being an incidental consequence of the correlation between σ_{sph} and M_{sph} .

4. INTRINSIC SCATTER IN THE $m_{\text{bh}}-\sigma_{\text{sph}}$ RELATION AND MODELS FOR SMBH EVOLUTION

In the previous section we showed that the observed scatter in the $M_{\text{bh}}-\sigma_{\text{sph}}$ and $M_{\text{bh}}-M_{\text{sph}}$ relations, when combined with the scatter among spheroid properties implies that the $M_{\text{bh}}-\sigma_{\text{sph}}$ relation is fundamental for SMBH growth, with the $M_{\text{bh}}-M_{\text{sph}}$ relation being incidental due to correlations between spheroid parameters. This in turn implies that if we have a model for the properties of the host spheroid, then we can deduce the mode of SMBH growth by comparing the calculated scatter in the modeled $M_{\text{bh}}-\sigma_{\text{sph}}$ and $M_{\text{bh}}-M_{\text{sph}}$ relations with observations. In this section we constrain the astrophysics of SMBH growth by computing minimum values for the scatter in the $M_{\text{bh}}-\sigma_{\text{sph}}$ relation using various models for the regulation of SMBH growth.

4.1. Rotation curves, Adiabatic cooling and the Fundamental Plane

Our goal is to model the scatter in the $M_{\text{bh}}-\sigma_{\text{sph}}$ and $M_{\text{bh}}-M_{\text{sph}}$ relations. To accomplish this goal we must have a representative model of the host spheroids as well as the scatter in their parameters. This is achieved by computing the rotation curve that results from cooling of baryons inside a dark-matter halo.

The virial radius R_{vir} and velocity V_{vir} for a halo of mass M_{halo} at redshift z are

$$R_{\text{vir}} = 109 \left(\frac{M_{\text{halo}}}{10^{12}M_{\odot}} \right)^{1/3} \left(\frac{\Omega_m}{\Omega_m^z} \frac{\Delta_c}{18\pi^2} \right)^{-1/3} \left(\frac{1+z}{2} \right)^{-1} \text{ kpc}, \quad (3)$$

and

$$V_{\text{vir}} = 200 \left(\frac{M_{\text{halo}}}{10^{12}M_{\odot}} \right)^{1/3} \left(\frac{\Omega_m}{\Omega_m^z} \frac{\Delta_c}{18\pi^2} \right)^{1/6} \left(\frac{1+z}{2} \right)^{1/2} \text{ km s}^{-1}, \quad (4)$$

where $\Omega_m^z \equiv [1 + (\Omega_{\Lambda}/\Omega_m)(1+z)^{-3}]^{-1}$, $\Delta_c = 18\pi^2 + 82d - 39d^2$ and $d = \Omega_m^z - 1$ (see Barkana & Loeb 2001 for more details). The relation of the circular velocity at the virial radius to the velocity dispersion at smaller galactic radii requires specification of the mass density profile. In this work we adopt the Navarro, Frenk & White (1997, hereafter NFW) profile for the dark matter. In addition to V_{vir} and M_{vir} the NFW profile is defined by the concentration parameter c , which is the ratio between the virial radius and a characteristic break radius, $c \equiv r_{\text{vir}}/r_s$. The median value of c depends on halo mass M_{halo} and redshift

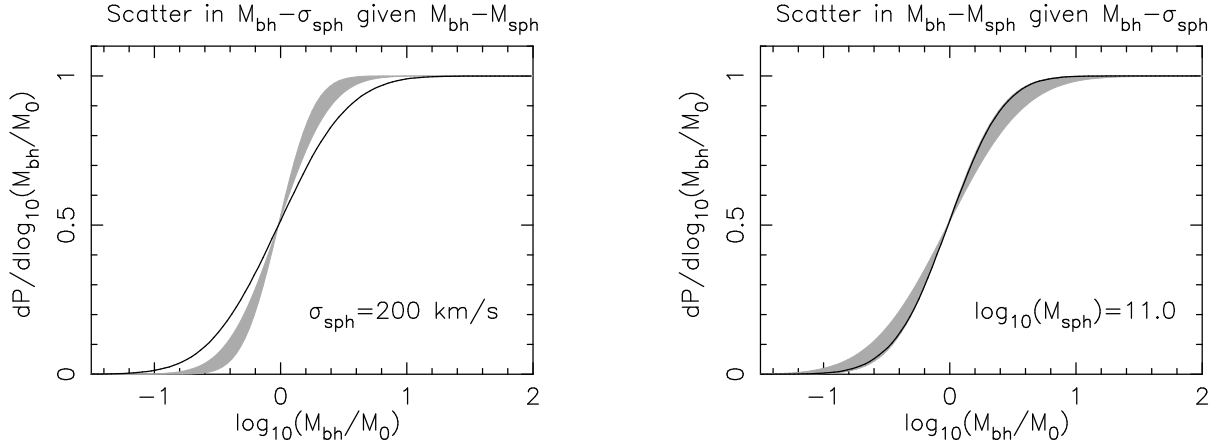


FIG. 1.— *Left*: The predicted intrinsic cumulative distribution of residuals ($\log_{10}(M_{\text{bh}}/M_0)$, where M_0 is the mass corresponding to the mean local relation) in M_{bh} at constant $\sigma_{\text{sph}} = 200 \text{ km s}^{-1}$. In this case the observed $M_{\text{bh}}-M_{\text{sph}}$ relation with intrinsic scatter of $\delta_{\text{sph}} = 0.41 \pm 0.07 \text{ dex}$ was assumed to be fundamental. *Right*: The predicted intrinsic residual scatter in the local M_{bh} at constant $M_{\text{sph}} = 10^{11} M_{\odot}$ assuming the observed $M_{\text{bh}}-\sigma_{\text{sph}}$ relation with intrinsic scatter of $\delta = 0.275 \pm 0.05 \text{ dex}$ to be fundamental. In each panel the range of the observed scatter (1-sigma) is shown as the shaded grey region for comparison. Zero scatter would have been represented by a step function.

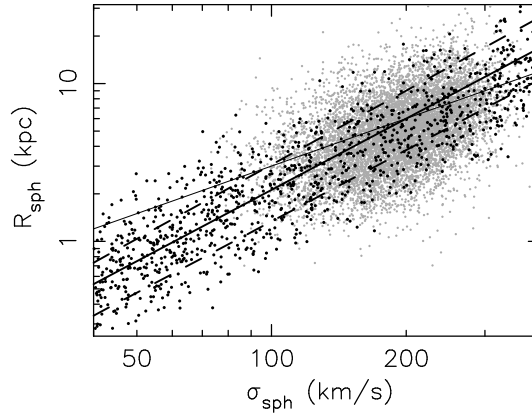


FIG. 2.— Scatter plot of R_{sph} vs σ_{sph} from cooled profiles inside dark matter halos (black-dots). For comparison, the SDSS sample (Bernardi et al. 2003) is shown by the grey dots. The thick solid and dashed lines show the mean observed relation $R_{\text{sph}} = 6(\sigma_{\text{sph}}/200)^{1.5}$ and the level of observed scatter ($\pm 0.2 \text{ dex}$). The thin solid line shows a linear relation.

z . Based on N-body simulations, Bullock et al. (2001) (see also Wechsler et al. 2002) have found a median relation for c ,

$$c = 7.3 \left(\frac{M_{\text{halo}}}{10^{12} M_{\odot}} \right)^{-0.13} \left(\frac{1+z}{2} \right)^{-1}, \quad (5)$$

with a scatter of $\Delta \log c = 0.14 \text{ dex}$.

The parameters describing the spheroid are its characteristic radius R_{sph} and velocity dispersion σ_{sph} . In this paper we assume that the gas available to cool in the halo makes most of the mass within the effective radius of the spheroid M_{sph} with a density distribution described by a Hernquist (1990) profile. The cooling of baryons modifies the density profile of a galaxy and hence its rotation curve. In particular, the velocity dispersion in the luminous portion of the galaxy is substantially larger than would be expected from an NFW profile. Gnedin et al. (2004) have studied the contraction of an NFW halo due to baryon cooling in a cosmological context. They find that traditional adiabatic contraction does not provide a good fit. However they introduce an alternative modified contraction model and provide fitting formulae for contracted pro-

files as a function of halo mass, concentration parameter, final characteristic radius for the baryons, and the cooled baryon fraction. From this contracted profile we can compute the velocity dispersion σ_{sph} at the characteristic radius R_{sph} . However the cooled profile, and hence the value of σ_{sph} obtained from the cooled profile depends on the value adopted for R_{sph} . Defining m_d to be the fraction of the total galaxy mass that makes the spheroid (including the cooled baryons), we can break this degeneracy by identifying the spheroid mass $m_d M_{\text{halo}}$ with the effective virial mass M_{sph} through $2\sigma_{\text{sph}}^2 R_{\text{sph}}/G = M_{\text{sph}} \equiv m_d M_{\text{halo}}$. With this second relation we are able to solve uniquely for R_{sph} and σ_{sph} within a specified dark matter halo (with parameters M_{halo} , c , z , and m_d). We choose a probability distribution that is flat in the logarithm of m_d over the range $0.015 \leq m_d \leq 0.15$. The upper value corresponds to the case where all baryons in the halo cool to form the mass of the spheroid [so that $M_{\text{sph}} = (\Omega_b/\Omega_m)M_{\text{halo}}$], and the range under consideration spans values smaller by up to an order of magnitude relative to this extreme case. Using this formalism we generate a sample of model spheroids. This sample is compared first to the observed fundamental

plane of early-type galaxies (below), and then used to discuss the scatter in models for the $M_{\text{bh}}-\sigma_{\text{sph}}$ and $M_{\text{bh}}-M_{\text{sph}}$ relations (§ 4.2).

Figure 2 shows a scatter plot of R_{sph} vs σ_{sph} for cooled profiles with randomly selected parameters. The distribution of formation redshift is dictated by the merger trees of halos and corresponding fate of pre-existing galaxies within these halos (Eisenstein & Loeb 1996). It is known empirically that star formation is rather minimal between $0 < z < 1$ for elliptical galaxies (Bernardi et al. 2003). Since we find that the relation between R_{sph} and σ_{sph} is not very sensitive to the precise probability distribution of collapse redshifts, we adopt in this figure a distribution of collapse redshifts that is flat between $1 < z < 3$. The resulting points show a correlation with significant scatter. For comparison, the relation between the velocity dispersion σ_{sph} of an early type stellar system and its effective radius R_e for galaxies from the SDSS (Bernardi et al. 2003) is shown by the grey dots. A fit to this observed correlation has the form

$$\log\left(\frac{R_e}{6\text{kpc}}\right) \approx 1.5 \log\left(\frac{\sigma_{\text{sph}}}{200\text{km s}^{-1}}\right), \quad (6)$$

which is plotted as the thick solid line in Figure 2. The scatter about the observed relation, $\pm 0.2\text{dex}$, is bracketed by the pair of dashed lines. Also plotted to guide the eye is a linear relation (thin line). On comparison with the results of Bernardi et al. (2003), we see that the formalism reproduces the observed behavior $R_{\text{sph}} \propto \sigma_{\text{sph}}^{1.5}$. Moreover the size of the predicted scatter about the mean relation is $\sim 0.17\text{dex}$, in good agreement with the observed value of $\sim 0.2\text{dex}$. This result is not very sensitive to the (unknown) distribution chosen for m_d . The model does not contain any free parameters. Nevertheless, in addition to the scatter an power-law slope of the $R_{\text{sph}}-\sigma_{\text{sph}}$ relation, our prescription also predicts its normalization.

For completeness we note that the relation described by equation (6) depends only on dynamical properties and not on the details of star-formation. However elliptical galaxies follow a 3-parameter *fundamental plane*, with the scatter around the median $R_{\text{sph}}-\sigma_{\text{sph}}$ relation parameterized by surface brightness rather than a 2 parameter relation (Djorgovski & Davis 1987). The scatter around the *fundamental plane* is substantially smaller than around the $R_{\text{sph}}-\sigma_{\text{sph}}$ relation shown in Figure 2. Bernardi et al (2003) find that the fundamental plane has the form

$$R_{\text{sph}} \propto \sigma_{\text{sph}}^{1.49 \pm 0.05} I_{\text{sph}}^{-0.75 \pm 0.01}, \quad (7)$$

where the surface brightness is $I_{\text{sph}} \propto L/R_{\text{sph}}^2$, and show that this requires the mass-to-light Γ to have a dependence on R_{sph} of the form $\Gamma \propto R_{\text{sph}}^{1/3}$. A complete model of the *fundamental plane* would need to explain this dependence of the mass-to-light ratio, in addition to the relation $R_{\text{sph}} \propto \sigma_{\text{sph}}^{1.5}$. However we do not expect SMBH growth to depend on Γ , and do not attempt to model this (orthogonal) parameter.

Finally, we note that the non-linearity of the relation between $R_{\text{sph}} \propto \sigma_{\text{sph}}^{1.5}$ is surprising since it is derived within the context of CDM dark-matter halos for which the relation between the virial radius and velocity is $R_{\text{vir}} \propto V_{\text{vir}}$ at any given redshift. In the following section we discuss the growth of SMBHs inside host spheroids in light of the observed scatters in the $M_{\text{bh}}-\sigma_{\text{sph}}$ and $M_{\text{bh}}-M_{\text{sph}}$ relations.

4.2. Models for SMBH Evolution

Three observations of the relation between SMBHs and their hosts have motivated different classes of models to describe the growth and evolution of SMBHs through accretion. First, the observation of the Magorrian et al. (1998) relation that the mass of the SMBH follows the mass of the spheroid has motivated models where the mass of the SMBH accretes a constant fraction of the available gas following a major merger (e.g. Haiman & Loeb 1998; Kauffmann & Haehnelt 2000). We refer to this scenario as case-I. Second, the observation of the $M_{\text{bh}}-\sigma_{\text{sph}}$ relation implies that the SMBH growth is regulated by the depth of the gravitational potential well of its host spheroid. We refer to this scenario as case-II. Third, there is evidence from the observation of the $M_{\text{bh}}-\sigma_{\text{sph}}$ relation in quasars, that the $M_{\text{bh}}-\sigma_{\text{sph}}$ relation does not vary with redshift (Shields et al. 2003). This motivates a revision of case-II, to include regulation of the SMBH growth over the dynamical time of the system (e.g. Silk & Rees 1998; Haehnelt, Natarajan & Rees 1998; Wyithe & Loeb 2003). We refer to this as case-III. On the other hand if momentum rather than energy is conserved in the transfer of energy in a quasars outflow to the cold galactic gas, then rather than a SMBH regulated by binding energy, we have a SMBH mass regulated by the binding energy divided by the virial velocity (Silk & Rees 1998; King 2003; Begelman 2004; Murray, Quataert, & Thompson 2005). In analogy with cases-II and III, the SMBH mass may be regulated by the total momentum of the surrounding gas, or by the total momentum divided by the systems dynamical time. We refer to these as cases-IV and V, respectively.

We therefore test five hypotheses for each of the $M_{\text{bh}}-\sigma_{\text{sph}}$ and $M_{\text{bh}}-M_{\text{sph}}$ relations. In the previous section we described a model that reproduces the observed behavior of $R_{\text{sph}} \propto \sigma_{\text{sph}}^{1.5}$, with a scatter of $\sim 0.2\text{dex}$. The agreement with the observed projection of the fundamental plane (Bernardi et al. 2003), gives us confidence that the model provides a sufficiently accurate framework within which we can discuss the scatter in the $M_{\text{bh}}-\sigma_{\text{sph}}$ and $M_{\text{bh}}-M_{\text{sph}}$ relations. Below we list the details of all cases under consideration:

- Case-I: the mass of the SMBH saturates at a constant fraction of the mass of the spheroid, $M_{\text{bh}} \propto M_{\text{sph}} \propto \sigma_{\text{sph}}^2 R_{\text{sph}}$.
- Case-II: the mass of the black-hole grows in proportion to the binding energy of baryons in the spheroid. Taking a constant fraction of the cold-gas mass to be material that must be expelled from the spheroid during the feedback we find that the black-hole mass is therefore $M_{\text{bh}} \propto M_{\text{sph}} \sigma_{\text{sph}}^2 \propto \sigma_{\text{sph}}^4 R_{\text{sph}}$.
- Case-III: the mass of the SMBH is determined by the mass for which accretion at the Eddington limit provides a constant fraction of the binding energy of the baryons in the spheroid over a constant fraction of the spheroid's dynamical time. Thus, the black-hole mass scales as $M_{\text{bh}} \propto E_b / (R_{\text{sph}} / \sigma_{\text{sph}}) \propto M_{\text{sph}} \sigma_{\text{sph}}^3 / R_{\text{sph}} \propto \sigma_{\text{sph}}^5$.

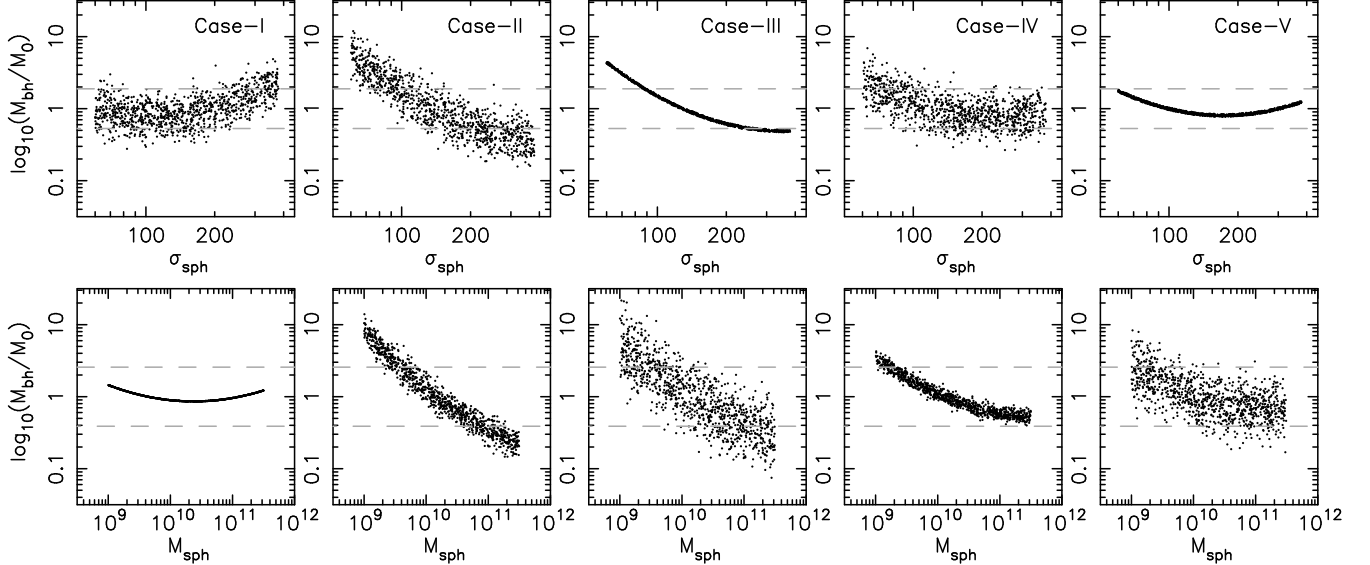


FIG. 3.— Predicted residual scatter ($\log_{10}(M_{\text{bh}}/M_0)$, where M_0 is the SMBH mass corresponding to the mean relation) relative to the best-fit log-quadratic relations. Results are shown as a function of σ_{sph} (upper row) and M_{sph} (lower row) for models where the SMBH growth is regulated by properties of the spheroid. The dashed grey lines show the level of observed scatter.

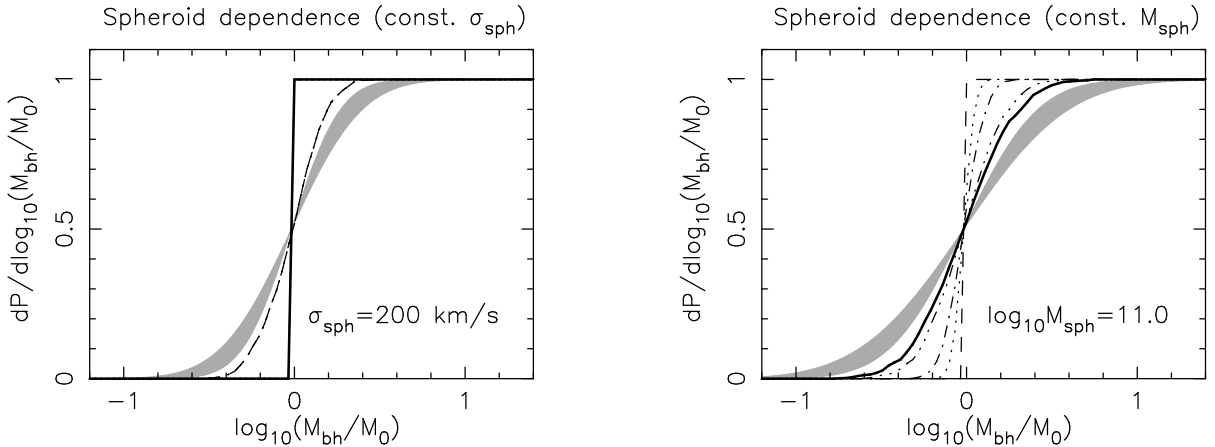


FIG. 4.— Predicted intrinsic scatter for models where the SMBH growth is regulated by properties of the spheroid. In each case we show the predicted cumulative distribution of residuals ($\log_{10}(M_{\text{bh}}/M_0)$, where M_0 is the SMBH mass corresponding to the mean relation) at constant $\sigma_{\text{sph}} = 200 \text{ km/s}$ (left) and constant $M_{\text{sph}} = 10^{11} M_{\odot}$ (right). The dashed, dot-dashed, solid, dotted, and dot-dot-dot lines correspond to cases I, II, III, IV and V respectively. In the left panel the lines for cases-III and V, and for cases-I, II and IV are coincident. In each panel the range of the observed scatter (1-sigma) is shown as the shaded grey region for comparison.

- Case-IV: As in case-II, but with the momentum rather than the energy of the outflow coupling to the gas in the spheroid, yielding $M_{\text{bh}} \propto M_{\text{sph}} \sigma_{\text{sph}} \propto \sigma_{\text{sph}}^3 R_{\text{sph}}$.
- Case-V: As in case-III, but with the momentum rather than the energy of the outflow coupling to the gas in the spheroid over a dynamical time, yielding $M_{\text{sph}} \sigma_{\text{sph}}^2 / R_{\text{sph}} \propto \sigma_{\text{sph}}^4$.

Studies of the local SMBH inventory suggest that most of mass in SMBHs was accreted during a luminous quasar phase (e.g. Yu & Tremaine 2002; Shankar et al. 2004), with a potentially significant contribution from an additional dust-obscured accretion phase (Martinez-Sansigre et al. 2005). If the fraction of obscured quasars is independent of redshift, then the quasar luminosity function (Fan et al. 2004; Boyle et al. 2000) can be used as a proxy

for the distribution of SMBH formation redshifts. Using this redshift distribution and the formalism outlined in the previous sub-section, we can estimate the slope and scatter in the $M_{\text{bh}}-\sigma_{\text{sph}}$ and $M_{\text{bh}}-M_{\text{sph}}$ relations under the five different scenarios for the regulation of SMBH growth.

For each of the five cases we perform Monte-Carlo simulations of SMBH growth. The resulting residuals in the $M_{\text{bh}}-\sigma_{\text{sph}}$ and $M_{\text{bh}}-M_{\text{sph}}$ relations are plotted in Figure 3 relative to the best fit log-quadratic relations (equations 1-2) as a function of σ_{sph} (upper row) and M_{sph} (lower row) respectively. For each of the five cases, we also compute distributions of residuals (in dex) relative to the mean SMBH mass at constant σ_{sph} and constant M_{sph} . The resulting distributions are plotted in Figure 4. The values of scatter are listed in the 1st and 2nd columns of Table 1. The ratio of the scatter at constant M_{sph} and at constant σ_{sph} are listed in column 3. The power-law slopes β and β_{sph} in each case are listed in columns 4 and 5.

TABLE 1

PREDICTED SCATTER AND LOGARITHMIC SLOPE IN THE $M_{\text{bh}}-\sigma_{\text{sph}}$ RELATION AND THE $M_{\text{bh}}-M_{\text{sph}}$ RELATION.

	spheroid					halo				
	δ	δ_{sph}	$\delta_{\text{sph}}/\delta$	β	β_{sph}	δ	δ_{sph}	$\delta_{\text{sph}}/\delta$	β	β_{sph}
Case-I	0.17 (0.275)	0.0 (0.22)	0 (0.8)	3.4	1.0	0.24 (0.275)	0.29 (0.31)	1.2 (1.1)	3.3	1.0
Case-II	0.17 (0.275)	0.10 (0.24)	0.6 (0.87)	5.3	1.6	0.36	0.48	1.3	5.4	1.6
Case-III	0.0 (0.275)	0.25 (0.37)	∞ (1.35)	5.0	1.5	0.37	0.53	1.4	5.5	1.5
Case-IV	0.17 (0.275)	0.05 (0.22)	0.29 (0.8)	4.2	1.3	0.39	0.38	1.0	4.3	1.3
Case-V	0.0 (0.275)	0.20 (0.34)	∞ (1.24)	4.0	1.2	0.29	0.42	1.4	4.4	1.3

From the above discussion we see that under the assumption of a unique coupling efficiency between the quasar output and the surrounding spheroid, cases-III and V imply a perfect $M_{\text{bh}}-\sigma_{\text{sph}}$ relation. Cases-I, II and IV do not produce perfect $M_{\text{bh}}-\sigma_{\text{sph}}$ relations even under this unique coupling assumption due to the scatter in the $R_{\text{sph}}-\sigma_{\text{sph}}$ relation. Similarly, the scatter in the $R_{\text{sph}}-\sigma_{\text{sph}}$ relation leads to scatter in the $M_{\text{bh}}-M_{\text{sph}}$ relation for cases-III and V. As a result, cases-III and V predict a scatter in the $M_{\text{bh}}-M_{\text{sph}}$ relation that is larger than in the $M_{\text{bh}}-\sigma_{\text{sph}}$ relation, in agreement with observations.

Obviously in these five cases we have neglected many additional sources of scatter. These include, but are not limited to, the fraction of the Eddington limit at which the SMBH shines during its luminous phase, the efficiency of coupling of feedback energy or momentum to the gas in the host spheroid, and the fraction of the system's characteristic size for which the dynamical time should be computed. In all five cases the minimum values of the scatter are smaller than the observed $\delta = 0.275$. However in cases I, II and IV, the models predict a scatter in the $M_{\text{bh}}-M_{\text{sph}}$ relation that is smaller than in the $M_{\text{bh}}-\sigma_{\text{sph}}$ relation while the observations show the opposite. On the other hand if SMBHs are regulated by the binding energy or momentum of gas in the spheroid per dynamical time of the spheroid (cases III & V), then the minimum scatter in the $M_{\text{sph}}-\sigma_{\text{sph}}$ relation is reduced to zero. Cases-III and V therefore predict that the scatter in the $M_{\text{bh}}-M_{\text{sph}}$ relation should be larger than in the $M_{\text{bh}}-\sigma_{\text{sph}}$ relation as observed.

The scatter in the projection of the fundamental plane onto the $R_{\text{sph}}-\sigma_{\text{sph}}$ plane therefore allows us to differentiate between SMBH growth that is regulated by the mass (Case-I), binding energy (Case-II) or momentum of gas (Case-IV) in the spheroid, and SMBH growth that is regulated by energy or momentum feedback over a dynamical time of the spheroid (Cases-III and V). In the latter cases the scatter in the $M_{\text{bh}}-M_{\text{sph}}$ relation is increased by the large scatter in the spheroid radius, R_{sph} . On the other hand in Cases-III and V, R_{sph} cancels out in the division of mass by dynamical time in the determination of M_{bh} at constant σ_{sph} .

If the predicted value for the minimum scatter in the $M_{\text{bh}}-\sigma_{\text{sph}}$ relation is smaller than the observed value of $\delta = 0.275$ dex, then there is room in the model for additional random scatter to account for varying Eddington ratio, outflow geometry, dust composition, and other factors. In each case we therefore add random scatter in the formation process at a level which results in the predicted scatter in the $M_{\text{bh}}-\sigma_{\text{sph}}$ relation being equal to the ob-

served value of $\delta = 0.275$ dex. This value, the corresponding value predicted for the scatter in the $M_{\text{bh}}-M_{\text{sph}}$ relation (δ_{sph}), and the corresponding ratio ($\delta_{\text{sph}}/\delta$) are listed in parentheses in Table 1. While cases-I, II and IV predict ratios of scatter between the $M_{\text{bh}}-M_{\text{sph}}$ and $M_{\text{bh}}-\sigma_{\text{sph}}$ relation that are smaller than unity, case-III predicts a ratio of $\delta_{\text{sph}}/\delta \sim 1.4$, and case-V a ratio of $\delta_{\text{sph}}/\delta \sim 1.2$, in good agreement with the observed value ($\delta_{\text{sph}}/\delta = 1.5 \pm 0.35$). We therefore conclude that SMBH growth is likely regulated by feedback over the spheroid's dynamical time.

A further possible discriminant between models is the power-law slope of the $M_{\text{bh}}-\sigma_{\text{sph}}$ relations. Cases III & V, which satisfy constraints from the observed scatter in the $M_{\text{bh}}-\sigma_{\text{sph}}$ and $M_{\text{bh}}-M_{\text{sph}}$ relations, produce power-law $M_{\text{bh}}-\sigma_{\text{sph}}$ relations, with SMBH mass in proportion to the velocity dispersion raised to the fifth and fourth power respectively. This could be compared with the power-law value from Tremaine et al. (2002) of $\beta = 4 \pm 0.3$ for galaxies with $\sigma_{\text{sph}} \sim 200 \text{ km s}^{-1}$, a comparison which at first sight this appears to support case-V. However Wyithe (2005) has found evidence for a power-law slope that varies with σ_{sph} from $\beta \sim 4$ near $\sigma_{\text{sph}} \sim 200 \text{ km s}^{-1}$, to $\beta \sim 5$ near $\sigma_{\text{sph}} \sim 350 \text{ km s}^{-1}$ (see Eq. 1). The slope of the $M_{\text{bh}}-M_{\text{sph}}$ relation is observed to be close to unity (Haering & Rix 2004). Of the cases (III and V) that produce an acceptably small scatter for the $M_{\text{bh}}-\sigma_{\text{sph}}$ relation, we find that case-III yields $\beta_{\text{sph}} \sim 1.5$, while case-V leads to a value of $\beta_{\text{sph}} \sim 1.2$. However Wyithe (2005) also finds evidence for a varying power-law in the $M_{\text{bh}}-M_{\text{sph}}$ relation, though not at high significance.

Since the models described in this paper each predict power-law relations between M_{bh} and σ_{sph} , the residuals with respect to the log-quadratic fit therefore show curvature as a function of σ_{sph} . Cases-III and V both show a power-law slope that agrees with the best-fit relation at some values of σ_{sph} , which renders discrimination between models based on their predicted power-law slope difficult. It is beyond the scope of this paper to discuss detailed models of the $M_{\text{bh}}-\sigma_{\text{sph}}$ relation; however the observed curvature may point to a turn-over from momentum to energy conservation in the reaction between the outflow and surrounding gas. Alternatively, there could be a velocity dependent efficiency of feedback, which could change the slope of the relation. In summary, based on the observed values of $\delta = 0.275 \pm 0.05$, $\delta_{\text{sph}} = 0.41 \pm 0.07$, only models corresponding to Case-III or Case-V are acceptable. Examples of this class include the models of Silk & Rees (1998); Wyithe & Loeb (2003); King (2003), di Matteo et al. (2005), or Murray et al. (2005).

4.3. Additional scatter from dissipationless mergers after the quasar epoch

Our model computes the minimum scatter in the $M_{\text{bh}}-\sigma_{\text{sph}}$ relation during a time when the SMBH can grow via gas accretion. At late times a SMBH may find itself in an environment where there is no remaining cold gas. In this regime a merger of two galaxies will proceed via collisionless dynamics. The two SMBHs may coalesce once they enter the gravity-wave dominated regime, but since there is no cold gas the SMBH will not grow during a quasar phase. It would require detailed numerical simulations to discover whether or not the $M_{\text{bh}}-\sigma_{\text{sph}}$ relation holds following a collisionless merger. However, unlike the situation where feedback is still at work, in a collisionless merger the stellar spheroid is not sensitive to the existence of the SMBH (at least at radii comparable to R_{sph}). Moreover the total SMBH mass is nearly conserved as long as SMBH binaries coalesce due to interactions with the surrounding stars and the emission of gravitational radiation (Begelman, Blandford, & Rees 1980). The growth of the SMBH and the properties of the spheroid following a collisionless merger should be independent in the sense of the $M_{\text{bh}}-\sigma_{\text{sph}}$ relation. Thus, we would expect collisionless mergers to increase the scatter in the $M_{\text{bh}}-\sigma_{\text{sph}}$ relation, leaving our estimates of the minimum scatter intact.

N-body simulations of the behavior of stars as collisionless particles have been performed by Gao et al. (2004) who found that the inner mass density profile (interior to some fixed physical radius) is unaffected by mergers, implying that the velocity dispersion interior to any given radius remains the same after a merger. When two spheroids merge, their combined stars cover a larger radius (because their mass increases while the inner mass profile remains unchanged), and this changes the value of σ_{sph} . We may therefore use the fact that the inner profile remains invariant in order to estimate the scaling between R_{sph} and σ_{sph} in the regime where purely collisionless mergers occur. Based on the simulations of Gao et al. (2004), we assume a universal NFW mass profile for the total mass (dark matter+stars) irrespective of the merger history and find what mergers would do to the $M_{\text{bh}}-\sigma_{\text{sph}}$ relation when the total mass in stars and in SMBHs is conserved. If the inner density profile maintains the NFW shape of $\rho \propto 1/r$, then $\sigma_{\text{sph}}^2 \propto r \propto M_{\text{sph}}^{1/2}$, i.e. $M_{\text{sph}} \propto \sigma_{\text{sph}}^4$, similar to the Faber-Jackson (1976) projection of the fundamental plane of spheroids.

Collisionless mergers will change the average normalization of the $M_{\text{bh}}-\sigma_{\text{sph}}$ relation. To see why, suppose that we have N_{p} equal mass progenitors at redshift z , each with velocity dispersion $\sigma_{\text{sph,p}}$ and spheroid mass $M_{\text{sph,p}}$. At redshift z , the SMBHs obey $M_{\text{bh,p}} = C_{\text{p}} \sigma_{\text{sph,p}}^{\beta_{\text{p}}}$, where β_{p} is the slope and C_{p} is a constant. The final SMBH and spheroid masses at $z = 0$ are $M_{\text{bh,f}} = N_{\text{p}} M_{\text{bh,p}}$ and $M_{\text{sph,f}} = N_{\text{p}} M_{\text{sph,p}}$ respectively. Using the above scaling the final velocity dispersion is $\sigma_{\text{sph,f}} = \sigma_{\text{sph,p}} N_{\text{p}}^{1/4}$. We therefore find $M_{\text{bh,f}} = N_{\text{p}} M_{\text{bh,p}} = N_{\text{p}} C_{\text{p}} \sigma_{\text{sph,p}}^{\beta_{\text{p}}} = C_{\text{p}} N_{\text{p}}^{1-\beta_{\text{p}}/4} \sigma_{\text{sph,f}}^{\beta_{\text{p}}}$. Thus the normalization of the $M_{\text{bh}}-\sigma_{\text{sph}}$ relation at fixed σ_{sph} is changed by a factor $\sim N_{\text{p}}^{1-\beta_{\text{p}}/4}$ through collisionless mergers. Note that the slope of the $M_{\text{bh}}-\sigma_{\text{sph}}$ relation β_{p} is preserved if N_{p} is independent of σ_{sph} . However

the number of progenitors is a function of halo mass and redshift, and so the change in normalization could be a function of σ_{sph} .

In addition to changing the normalization of the $M_{\text{bh}}-\sigma_{\text{sph}}$ relation, collisionless mergers will also introduce scatter. In the limit of a perfect correlation between M_{sph} and σ_{sph} , and where the number of progenitors (N_{p}) is constant, the argument in the previous paragraph shows that collisionless mergers would lead to an $M_{\text{bh}}-\sigma_{\text{sph}}$ relation with no additional scatter beyond that introduced at the formation redshift. However the scatter in the $R_{\text{sph}}-\sigma_{\text{sph}}$ correlation combined with the relation $M_{\text{sph}} \propto \sigma_{\text{sph}}^2 R_{\text{sph}}$ implies that there is $\sim 0.2\text{dex}$ of scatter in M_{sph} at fixed σ_{sph} . Moreover, different galaxies have different merger histories and therefore a different number of progenitors. Scatter among the properties of the initial building blocks at redshift z therefore leads to scatter in the local $M_{\text{bh}}-\sigma_{\text{sph}}$ relation even if the $M_{\text{bh}}-\sigma_{\text{sph}}$ relation at z were perfect. This scatter introduced through collisionless mergers will therefore add scatter to the local $M_{\text{bh}}-\sigma_{\text{sph}}$ relation beyond that intrinsic to the formation process itself.

To ascertain the quantitative effect of collisionless mergers on scatter in the $M_{\text{bh}}-\sigma_{\text{sph}}$ relation, we generate merger trees of dark-matter halos using the method described in Vollonteri, Haardt & Madau (2003). Based on the merger trees we find the N_{p} progenitor halos at $z \sim 1.5$ that lead to a halo of known mass at $z \sim 0$. Using the formalism outlined in § 4.1 we then determine the values of σ_{sph} , R_{sph} and M_{sph} for the spheroids populating these progenitor halos. We also populate the spheroids with SMBHs of mass M_{bh} according to the perfect $M_{\text{bh}}-\sigma_{\text{sph}}$ relations that arise from cases-III and V. The final SMBH mass residing in the halo at $z = 0$ is $M_{\text{bh,f}} = \sum_{i=0}^{N_{\text{p}}} M_{\text{bh,i}}$. It is embedded in a spheroid of mass $M_{\text{sph,f}} = \sum_{i=0}^{N_{\text{p}}} M_{\text{sph,i}}$. Based on the above scaling for the inner $\rho \propto 1/r$ density profile of an NFW halo we may estimate the value of velocity dispersion corresponding to the final spheroid, $\sigma_{\text{sph,f}} = \sigma_{\text{sph,0}} (M_{\text{sph,f}}/M_{\text{sph,0}})^{1/4}$, where $M_{\text{sph,0}}$ and $\sigma_{\text{sph,0}}$ are the mass and velocity dispersion of the largest progenitor. In Figure 5 we show the scatter introduced into a perfect $M_{\text{bh}}-\sigma_{\text{sph}}$ relation originating at $z = 0.5$ (left), $z = 1.5$ (center) and $z = 2.5$ (right) by collisionless mergers between those redshifts and $z = 0$. As discussed above this scatter arises as a result of scatter in the relation between σ_{sph} and M_{sph} in the progenitors. The upper panels show results for Case-III ($\beta = 5$), while the lower panels show results for Case-V ($\beta = 4$). The scatter introduced is roughly independent of σ_{sph} and takes values of $\delta \sim 0.1\text{dex}$, $\delta \sim 0.2\text{dex}$ and $\delta \sim 0.3\text{dex}$ for mergers originating at $z = 0.5$, $z = 1.5$ and $z = 2.5$, respectively. Thus galaxies that become devoid of gas at higher redshift lead to a larger scatter in the $M_{\text{bh}}-\sigma_{\text{sph}}$ relation, because these galaxies undergo more collisionless mergers by $z = 0$ than a galaxy which becomes devoid of gas only at late times.

The stars that populate massive galaxies appear to be older than those in low mass galaxies (Kauffmann et al. 2003). The cold gas reservoir that made these stars must have been depleted at a higher redshift for the progenitors of high- σ_{sph} galaxies. We might therefore expect more scatter in the $M_{\text{bh}}-\sigma_{\text{sph}}$ relation at large σ_{sph} . For equal mass mergers we have shown that the normalization of the $M_{\text{bh}}-\sigma_{\text{sph}}$ relation at a fixed σ_{sph} changes by a factor

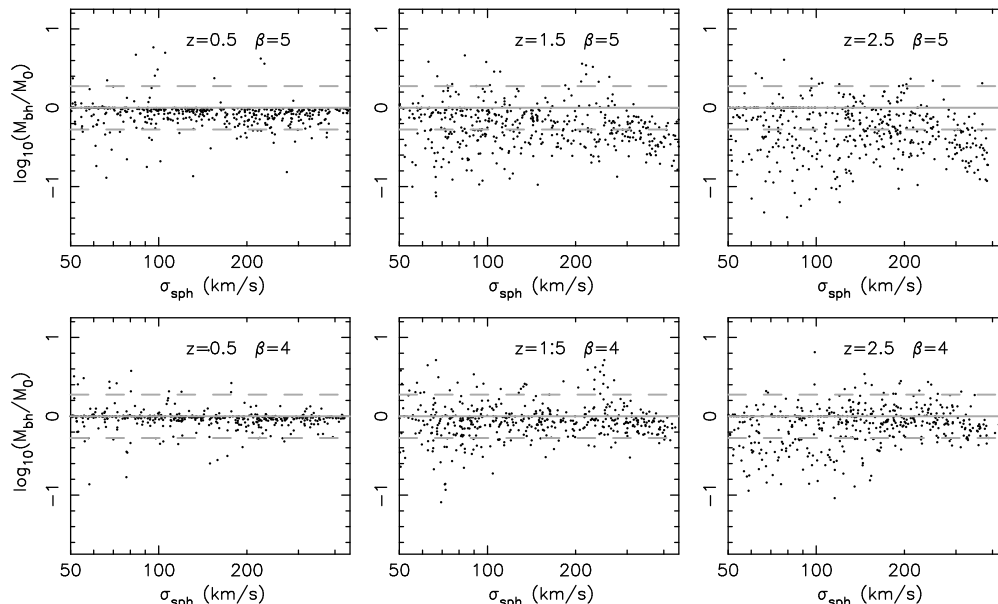


FIG. 5.— Scatter plots of the predicted residuals ($\log_{10}(M_{\text{bh}}/M_0)$, where M_0 is the SMBH mass corresponding to the mean power-law relation at redshift z) in M_{bh} that result from collisionless galaxy mergers. Each point represents a different realization of a collisionless merger tree beginning with a perfect power-law $M_{\text{bh}}-\sigma_{\text{sph}}$ correlation at $z = 0.5$ (left panel), $z = 1.5$ (center panel) and $z = 2.5$ (right panel). We assume Case-III $\beta = 5$ (upper row) and Case-V $\beta = 4$ (lower row).

$\sim N_p^{1-\beta_p/4}$. Thus, for $\beta_p = 5$ (Case-III), we find that the amplitude of the $M_{\text{bh}}-\sigma_{\text{sph}}$ relation should be reduced by collisionless mergers, while for $\beta_p = 4$ (Case-V) the amplitude should be preserved. This behavior is seen in Figure 5. Moreover, more massive galaxies undergo a larger rate of major mergers. Figure 5 shows that in Case-V the change in normalization of the $M_{\text{bh}}-\sigma_{\text{sph}}$ relation through collisionless mergers is more significant in high mass than in low mass galaxies, as expected. Collisionless mergers could therefore lead to a reduction in the steepness of the observed $M_{\text{bh}}-\sigma_{\text{sph}}$ relation if $\beta_p > 4$.

In summary, in order to satisfy the constraint that the $M_{\text{bh}}-\sigma_{\text{sph}}$ relation have a scatter at $z = 0$ that is smaller than $\sim 0.3\text{dex}$, the intrinsic scatter in the relation at the formation redshift should be smaller than $\sim 0.2\text{dex}$, so as to allow for the additional scatter introduced through collisionless mergers. Cases-III and V meet this requirement.

4.4. Redshift dependence of the $M_{\text{bh}}-\sigma_{\text{sph}}$ and $M_{\text{bh}}-M_{\text{sph}}$ relations

Recent evidence suggests that the $M_{\text{bh}}-\sigma_{\text{sph}}$ relation is preserved out to high redshift (Shields et al. 2003), while SMBHs make a larger fraction of their host spheroid mass at higher redshift (Rix et al. 2001; Croom et al. 2004; Walter et al. 2004). This behavior is reproduced in models with scenarios of the form case-III or case-V. Figure 6 shows a scatter plot of the predicted residuals in M_{bh} vs z at constant $\sigma_{\text{sph}} = 200\text{ km s}^{-1}$ (upper row) and $M_{\text{sph}} = 10^{11}M_{\odot}$ (lower row) for each of the five models. The residuals are normalized relative to the mean relation at $z = 3$ in each case. While there is no evolution in the $M_{\text{bh}}-\sigma_{\text{sph}}$ relation for cases-III and V, we see that SMBHs are predicted to be an order of magnitude more massive with respect to their host spheroid at $z \sim 6$ than they are at $z \sim 1$ in agreement with observations. In contrast, models for case-I, II and IV predict that the SMBH mass

should decrease by an order of magnitude between $z = 0$ and $z = 6$ at constant σ_{sph} , while not evolving significantly at constant M_{sph} . The observed evolution of SMBH mass with redshift therefore supports cases III and V as the scenario for SMBH growth. This result supports the findings of § 4.2 based on the scatter in local relations.

4.5. Do dark-matter halos play a role in SMBH evolution?

Attempts to reproduce the observed luminosity function of quasars associate the mass of the SMBH with the properties of the host dark-matter halo. This paradigm allows the abundance of SMBHs to be traced either in semi-analytic or numerical models (e.g. Haiman & Loeb 1998; Haehnelt, Natarajan & Rees 1998; Wyithe & Loeb 2003; Vollonteri, Haardt & Madau 2002). Indeed, Ferrarese (2001) has inferred a relation between the masses of SMBHs and their host dark-matter halo. *Is it possible that the halo rather than the spheroid regulates SMBH growth?*

Since we have computed spheroid properties within a specified dark matter halo, we are in a position to discuss the role of the dark matter halo in regulating the SMBH growth. In addition to the five cases listed above for SMBH growth within a spheroid, we also try five analogous cases for the formation of SMBHs governed by dark matter halo properties. For each of the additional five cases, we compute the distribution of residuals (in dex) relative to the mean relation as a function of σ_{sph} and M_{sph} via a Monte-Carlo algorithm for SMBH formation, and calculate the variance at each of constant $\sigma_{\text{sph}} = 200\text{ km s}^{-1}$ and constant $M_{\text{sph}} = 10^{11}M_{\odot}$. Below we list the details of each case. The resulting distributions of residuals are plotted in figure 7. The values of scatter are listed in the 6th and 7th columns of Table 1. The ratio of the scatter at constant M_{sph} and at constant σ_{sph} are listed in column 8. Values

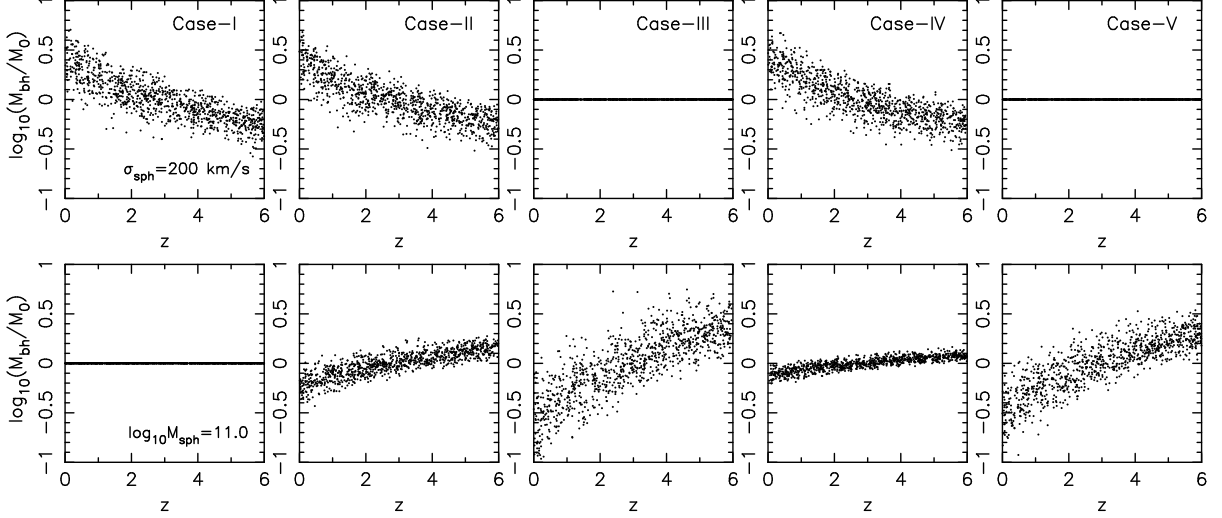


FIG. 6.— Scatter plots of the predicted residuals ($\log_{10}(M_{\text{bh}}/M_0)$, where M_0 is the SMBH mass corresponding to the mean relation) in M_{bh} as a function of z . Results are shown at constant $\sigma_{\text{sph}} = 200 \text{ km s}^{-1}$ (upper row) and constant $M_{\text{sph}} = 10^{11} M_{\odot}$ (lower row) for models where SMBH formation is governed by spheroid properties. In each of the five cases shown the residuals are relative to the mean relation at $z = 3$.

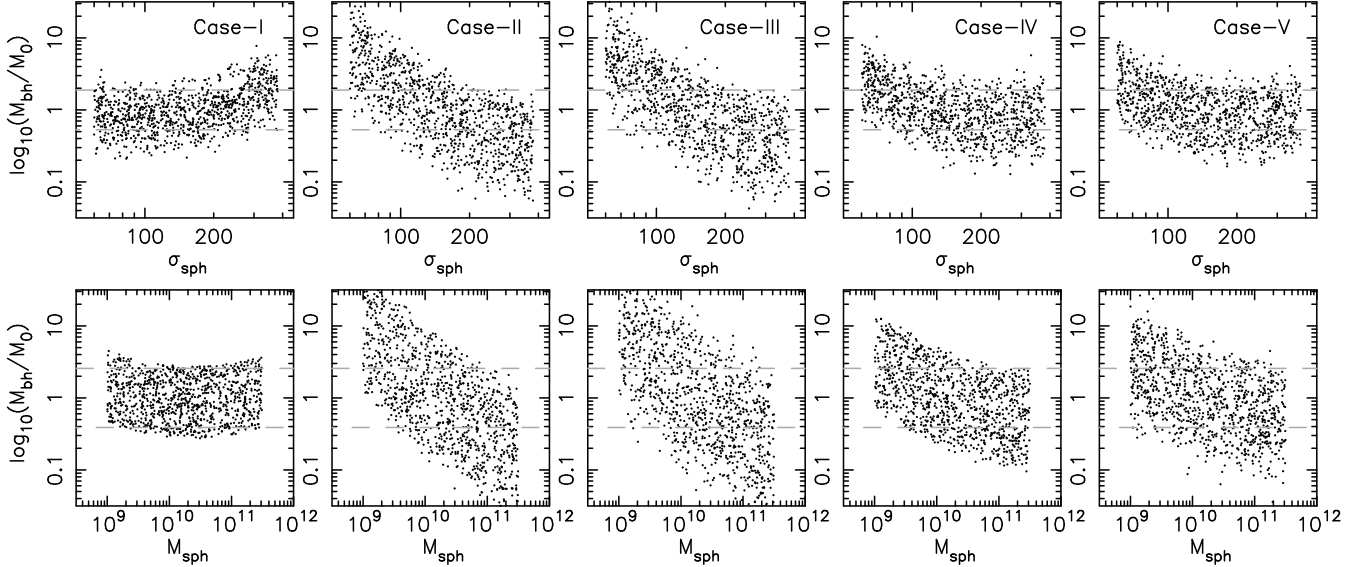


FIG. 7.— Predicted scatter of residuals ($\log_{10}(M_{\text{bh}}/M_0)$ where M_0 is the SMBH mass corresponding to the mean relation) relative to the best-fit log-quadratic relations. Results are shown as a function of σ_{sph} (upper row) and M_{sph} (lower row) for models where the SMBH growth is regulated by properties of the dark matter halo. The dashed grey lines show the level of observed scatter.

for the slopes β and β_{sph} are listed in columns 9 and 10.

- Case-I: the mass of the SMBH forms from a constant fraction of the baryonic component of the halo mass, $M_{\text{bh}} \propto (\Omega_{\text{b}}/\Omega_{\text{m}})M_{\text{halo}}$.
- Case-II: the mass of the black-hole grows in proportion to the binding energy of baryons in the halo. For an NFW profile with a concentration parameter c we get $M_{\text{bh}} \propto (\Omega_{\text{b}}/\Omega_{\text{m}})M_{\text{halo}}V_{\text{vir}}^2 f_c$, where
$$f_c = \frac{c}{2} \frac{1 - 1/(1+c)^2 - 2\ln(1+c)/(1+c)}{[c/(1+c) - \ln(1+c)]^2}. \quad (8)$$
- Case-III: the mass of the SMBH is determined by the mass for which accretion at the Eddington limit provides the binding energy of baryons in the halo over a constant fraction of the halo's dynamical

time (Wyithe & Loeb 2003). We therefore have $M_{\text{bh}} \propto \frac{(\Omega_{\text{b}}/\Omega_{\text{m}})M_{\text{halo}}V_{\text{vir}}^2 f_c}{R_{\text{vir}}/V_{\text{vir}}} \propto f_c V_{\text{vir}}^5$.

- Case-IV: same as case-II, but with the momentum rather than the energy of the outflow coupling to the gas in the spheroid. We then find $M_{\text{bh}} \propto (\Omega_{\text{b}}/\Omega_{\text{m}})M_{\text{halo}}V_{\text{vir}}f_c$
- Case-V: same as case-IV, but with the momentum rather than the energy of the outflow coupling to the gas in the spheroid over a dynamical time. We then find $M_{\text{bh}} \propto \frac{(\Omega_{\text{b}}/\Omega_{\text{m}})M_{\text{halo}}V_{\text{vir}}f_c}{R_{\text{vir}}/V_{\text{vir}}} \propto f_c V_{\text{vir}}^4$.

In these five cases we have again neglected many possible causes of scatter. However in case-I, where the SMBH growth is regulated by halo properties, the minimum value

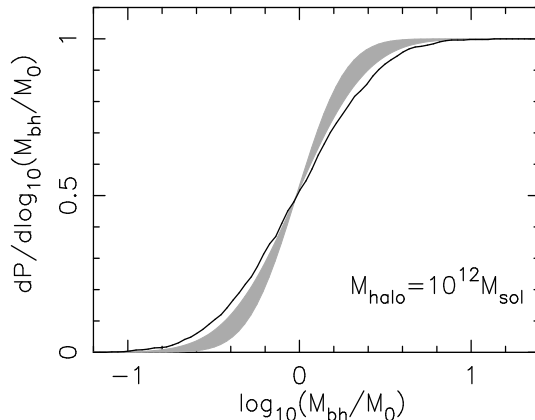


FIG. 8.— The predicted distribution of intrinsic residuals ($\log_{10}(M_{\text{bh}}/M_0)$ where M_0 is the SMBH mass corresponding to the mean relation) in the local M_{bh} at $M_{\text{halo}} = 10^{12} M_{\odot}$. The $M_{\text{bh}}-M_{\text{halo}}$ relation has larger intrinsic scatter than the $M_{\text{bh}}-\sigma_{\text{sph}}$ relation.

of the scatter in the $M_{\text{bh}}-\sigma_{\text{sph}}$ relation is slightly smaller than the observed $\delta = 0.275$. We have added random scatter to the model for case-I in order to bring the predicted scatter in the $M_{\text{bh}}-\sigma_{\text{sph}}$ up to the observed value. This value and the corresponding prediction for δ_{sph} and $\delta/\delta_{\text{sph}}$ are listed in parentheses. Case-I predicts a scatter in the $M_{\text{bh}}-M_{\text{sph}}$ relation that is similar to the $M_{\text{bh}}-\sigma_{\text{sph}}$ relation while the observations suggest the latter to be significantly smaller. While case-I cannot be ruled out based only on the predicted minimum scatter in the $M_{\text{bh}}-\sigma_{\text{sph}}$ relation at the formation redshift, the small allowance for additional expected scatter from the aforementioned astrophysical sources renders it unlikely, particularly when the additional scatter of $0.1-0.3\text{dex}$ from collisionless mergers at low redshift is accounted for. In cases II, III, IV and V where the SMBH growth is regulated by halo properties, the minimum values of the scatter in the $M_{\text{bh}}-\sigma_{\text{sph}}$ relation are larger than the observed $\delta = 0.275$.

While scatter within models of spheroid regulated SMBH growth is not sensitive to the distribution of m_{d} , the predicted scatter in models of halo regulated SMBH growth decreases as the assumed range of m_{d} decreases. However, in order to reduce the predicted scatter below the $\sim 0.2\text{dex}$ threshold at the formation redshift (which would allow for additional scatter to be introduced through collisionless mergers), we find that the allowed range around $m_{\text{d}} = 0.05$ would need to be smaller than ± 0.025 , which is implausibly narrow. We therefore conclude that it is the spheroid rather than the dark-matter halo which drives the evolution of SMBH mass.

4.6. The $M_{\text{bh}}-M_{\text{halo}}$ relation

We have demonstrated that the tight relation between M_{bh} and σ_{sph} implies that it is the spheroid rather than the halo which governs the growth of SMBHs. However it is clear that since there is an $M_{\text{bh}}-\sigma_{\text{sph}}$ relation, and since larger halos will, on average, host bulges with larger central velocity dispersions, there should also be a correlation between SMBH and halo mass. Ferrarese (2001) has found such a relation. Since it is not possible to measure the dark matter halo mass directly, halo masses for galaxies in the local sample were inferred via a maximum circular velocity estimated from σ_{sph} based on an empirical relation. It is therefore difficult to estimate the scatter in the $M_{\text{bh}}-$

M_{halo} relation observationally. Here we predict the scatter in the $M_{\text{bh}}-M_{\text{halo}}$ relation at a fixed value of M_{halo} . We compute the distribution of residuals via a Monte-Carlo method as before. We choose $M_{\text{halo}} = 10^{12} M_{\odot}$ and find the distribution of values for σ_{sph} , and hence the distribution of M_{bh} using the observed $M_{\text{bh}}-\sigma_{\text{sph}}$ relation. The resulting distribution is plotted in Figure 8. The variance is $\delta_{\text{halo}} = 0.4\text{ dex}$. Thus the tightness of the $M_{\text{bh}}-\sigma_{\text{sph}}$ relation suggests that the $M_{\text{bh}}-M_{\text{halo}}$ correlation is incidental to the fundamental relation between the SMBH and its host spheroid. Note that this variance is computed at the time of the SMBH formation. The surrounding dark matter halo could continue to grow after the supply of cold gas to the SMBH had ceased. This is consistent with our conclusion that SMBHs grow in proportion to the properties of the spheroid rather than the halo. Indeed one finds massive dark-matter halos in X-ray clusters, which must have increased their velocity dispersion well beyond the corresponding SMBH growth (due to the lack of cooling flows in cluster cores). This late-time growth of dark-matter halos increases considerably the scatter in the $M_{\text{bh}}-M_{\text{halo}}$ relation.

5. CONCLUSION

We have investigated the implications of intrinsic scatter in the local relations involving SMBHs for models of SMBH formation. Using the sample of spheroid properties from SDSS (Bernardi et al. 2003) we first examined empirically the fundamental parameter describing SMBH growth. The observed scatter in the $M_{\text{bh}}-\sigma_{\text{sph}}$ relation is $\delta = 0.275 \pm 0.05$, while the $M_{\text{bh}}-M_{\text{sph}}$ relation has a larger observed scatter of $\delta_{\text{sph}} = 0.41 \pm 0.07$. Assuming that the $M_{\text{bh}}-M_{\text{sph}}$ relation is fundamental, we use the SDSS spheroid sample to compute the resulting scatter in the $M_{\text{bh}}-\sigma_{\text{sph}}$ relation. We find that this procedure results in a scatter of the $M_{\text{bh}}-\sigma_{\text{sph}}$ relation that is too large to be reconciled with observation. Alternatively, one might assume that SMBH growth is determined by σ_{sph} rather than M_{sph} . In this case we used the SMBH sample to compute the resulting scatter in the $M_{\text{bh}}-M_{\text{sph}}$ relation, and found agreement with the observed scatter. We therefore conclude that SMBH growth is governed by σ_{sph} , and that the observed correlation between M_{bh} and M_{sph} is a by-product of the relation between M_{sph} and σ_{sph} .

Theoretical models for SMBH formation must reproduce several observational constraints: (i) the scatter in the local $M_{\text{bh}}-\sigma_{\text{sph}}$ relation is $\delta = 0.275 \pm 0.05$ dex, implying that at the time of formation the scatter should be smaller than ~ 0.2 dex to allow for additional scatter introduced by collisionless mergers of galaxies since $z \sim 1$ or earlier; (ii) the scatter in the $M_{\text{bh}}-M_{\text{sph}}$ relation is larger than in the $M_{\text{bh}}-\sigma_{\text{sph}}$ relation (this result is maintained as additional scatter from collisionless mergers is introduced after SMBH formation); and (iii) The $M_{\text{bh}}-\sigma_{\text{sph}}$ relation is preserved out to high redshift. We find that these constraints are only met by models where SMBH growth is regulated by feedback on the gas feeding the SMBH over the spheroidal dynamical time. Other models lead to scatter in the $M_{\text{bh}}-\sigma_{\text{sph}}$ relation that are too large or scatter in the $M_{\text{bh}}-M_{\text{sph}}$ relation that is smaller than the $M_{\text{bh}}-\sigma_{\text{sph}}$ relation. In addition, other models lead to a SMBH mass that drops with increasing redshift at a fixed velocity dispersion. The feedback in successful models can be either

in the form of energy or momentum transfer between the quasar and the galactic gas, leading to power-law slopes in the $M_{\text{bh}}-\sigma_{\text{sph}}$ relation of $\beta = 4$ or $\beta = 5$, respectively. Both of these slopes are permitted by the local sample (Wyithe 2005).

The above constraints do *not* permit SMBH growth to be governed by the properties of the dark-matter halos. Such models lead to scatter in the $M_{\text{bh}}-\sigma_{\text{sph}}$ relation that are too large and/or scatter in the $M_{\text{bh}}-M_{\text{sph}}$ relation that is smaller than the $M_{\text{bh}}-\sigma_{\text{sph}}$ relation. The relation between M_{bh} and the halo mass (Ferrarese 2001) has a large scatter (~ 0.4 dex) and is most likely a by-product of the correlation between halo mass and σ_{sph} .

J.S.B.W. acknowledges the support of the Australian Research Council. This work was supported in part by NASA grants NAG 5-13292, NNG-05-GH54G, and by NSF grants AST-0071019, AST-0204514 (for A.L.).

REFERENCES

- Adams, F. C., Graff, D. S., Mbonye, M., & Richstone, D. O. 2003, *ApJ*, 591, 125
- Barkana, R., Loeb, A. 2001, *Phys. Rep.*, 349, 125
- Begelman, M. C. 2004, *Coevolution of Black Holes and Galaxies*, 375
- Begelman, M. C., Blandford, R. D., & Rees, M. J. 1980, *Nature*, 287, 307
- Bernardi, M., et al. 2003, *Astron. J.*, 125, 1866
- Boyle, B. J., Shanks, T., Croom, S. M., Smith, R. J., Miller, L., Loaring, N., & Heymans, C. 2000, *MNRAS*, 317, 1014
- Bullock, J. S., Kolatt, T. S., Sigad, Y., Somerville, R. S., Kravtsov, A. V., Klypin, A. A., Primack, J. R., & Dekel, A. 2001, *MNRAS*, 321, 559
- Croom, S.M., Schade, D., Boyle, B.J., Shanks, T., Miller, L., Smith, R.J., 2004, *Astrophys. J.*, 606, 126
- Di Matteo, T., Springel, V., & Hernquist, L. 2005, *Nature*, 433, 604
- Djorgovski, S., & Davis, M. 1987, *ApJ*, 313, 59
- Eisenstein, D. J., & Loeb, A. 1996, *ApJ*, 459, 432
- Faber, S. M., & Jackson, R. E. 1976, *ApJ*, 204, 668
- Fan, X., et al. 2004, *AJ*, in press; astro-ph/0405138
- Ferrarese, L., & Merritt, D. 2000, *ApJ. Lett.*, 539, L9
- Ferrarese, L., 2001, *Astrophys. J.*, 587, 90
- Gao, L., Loeb, A., Peebles, P. J. E., White, S. D. M., & Jenkins, A. 2004, *ApJ*, 614, 17
- Gebhardt, K., et al. 2000, *ApJ. Lett.*, 539, L13
- Gnedin, O. Y., Kravtsov, A. V., Klypin, A. A., & Nagai, D. 2004, *ApJ*, 616, 16
- Graham, A. W., Erwin, P., Caon, N., & Trujillo, I. 2002, *Astronomical Society of the Pacific Conference Series*, 275, 87
- Haehnelt, M. G., Natarajan, P., & Rees, M. J. 1998, *MNRAS*, 300, 817
- Haiman, Z., & Loeb, A. 1998, *ApJ*, 503, 505
- Häring, N., & Rix, H. 2004, *ApJ. Lett.*, 604, L89
- Hernquist, L. 1990, *ApJ*, 356, 359
- Kauffmann, G., & Haehnelt, M. 2000, *MNRAS*, 311, 576
- Kauffmann, G., et al. 2003, *MNRAS*, 341, 54
- King, A. 2003, *ApJ. Lett.*, 596, L27
- Kormendy, J., & Richstone, D. 1995, *Ann. Rev. Astron. Astrophys.*, 33, 581
- Magorrian, J., et al. 1998, *Astron. J.*, 115, 2285
- Martinez-Sansigre, A., Rawlings, S., Lacy, M., Fadda, D., Marleau, F.R., Simpson, C., Willott, C.J., Jarvis, M.J., 2005, astro-ph/0505486
- Miralda-Escudé, J., & Kollmeier, J. A. 2005, *ApJ*, 619, 30
- Murray, N., Quataert, E., & Thompson, T. A. 2005, *ApJ*, 618, 569
- Navarro, J. F., Frenk, C. S., & White, S. D. M. 1997, *ApJ*, 490, 493
- Rix, H.-W., Falco, E. E., Impey, C., Kochanek, C., Lehar, J., McLeod, B., Muñoz, J., & Peng, C. 2001, *ASP Conf. Ser.* 237: *Gravitational Lensing: Recent Progress and Future Go*, 237, 169
- Robertson, B., Hernquist, L., Cox, T.J., Di Matteo, T., Hopkins, P.F., Martini, P., Springel, V., 2005, astro-ph/0506038
- Sazonov, S. Y., Ostriker, J. P., Ciotti, L., & Sunyaev, R. A. 2005, *M.N.R.A.S.*, 358, 168
- Shankar, F., Salucci, P., Granato, G. L., De Zotti, G., & Danese, L. 2004, *M.N.R.A.S.*, 354, 1020
- Shields, G. A., Gebhardt, K., Salvander, S., Wills, B. J., Xie, B., Brotherton, M. S., Yuan, J., & Dietrich, M. 2003, *ApJ*, 583, 124
- Silk, J., & Rees, M. J. 1998, *Astron. Astrophys.*, 331, L1
- Spergel, D. N., et al. 2003, *AJ Supp.*, 148, 175
- Tremaine, S., et al. 2002, *ApJ*, 574, 740
- Volonteri, M., Haardt, F., & Madau, P. 2003, *ApJ*, 582, 559
- Walter, F., Carilli, C., Bertoldi, F., Menten, K., Cox, P., Lo, K. Y., Fan, X., & Strauss, M. A. 2004, *ApJ*, 615, L17
- Wechsler, R. H., Bullock, J. S., Primack, J. R., Kravtsov, A. V., & Dekel, A. 2002, *ApJ*, 568, 52
- Wyithe, J. S. B., & Loeb, A. 2003, *ApJ*, 595, 614
- Wyithe, J. S. B., 2005, astro-ph/0503435
- Yu, Q., Tremaine, S., 2002, *MNRAS*, 335, 965